

Unconventional exploration of failure modes in rock and rock masses

N.R. Barton

NB&A, Oslo, Norway
nickrbarton@hotmail.com

Abstract

This paper deals with the exploration of failure modes in rock and rock masses, starting with extension failure in deep tunnels, followed by analysis of the limited heights of cliffs, mountain walls and mountains. Here, tensile failure applies to the cliffs and mountain walls, since cohesive strength is too high, and shear strength applies to the maximum mountain heights since confined compression strength is too high. In each case it is the weakest link that applies, as in morphological processes.

The actual strength of rock masses is neither Mohr-Coulomb nor Hoek-Brown nor friction coefficient based, although the latter may be useful for describing the more linear residual strength of faults. We should not be adding ' $c + \sigma_n \tan \varphi$ ' since these components are not mobilized in unison. Intact rock has a cohesive strength that is so high that it makes mountain avalanches rare events. Frictional strength tends to be high as well, due to the big additional contribution of fracture dilation. The weakest link of the intact rock is of course the tensile strength, and this is proved by cliff height limits in a wide range of rock types with heights varying by a factor of 100 depending mostly on tensile strength.

Thanks to recent work by Baotang Shen it is now known that Poisson's ratio plays a major role in initial failure, as even rock under 3D compression can fail in tension due to the mechanism of extensional strain in the direction of a nearby free surface. This is an important morphological property. At higher stress levels, the extensional fractures may propagate in shear.

A simple new cliff formula is demonstrated based on tensile strength, density and Poisson's ratio. Naturally if the rock is jointed, there are usually massive changes in strength and stability and slope height, in relation to slopes in intact rock. Failure may be progressive in nature, involving several components of strength which are mobilized at different shear displacements or strains. The stability of the famous Prekestolen in SW Norway will be assessed from a new viewpoint, considering several components of strength and including potential extension strain-based failure at its base. It's factor of safety may be different from that obtained by conventional shear strength analysis.

The apparent 8 to 9km height limit of mountains, of course lower than this below the immediate peaks, will be addressed using critical state shear strength arguments, since confined compression strength is too high. The strongly non-linear nature of shear strength is emphasised throughout. Non-linearity is stronger than Hoek-Brown. Maximum shear strength is numerically similar to UCS and this has probably confused popular analysis of height limits which have been based on UCS.

Keywords Shear strength, tensile strength, extension, tunnels, cliffs, mountains



1 Introduction

This paper deals with the exploration of failure modes in rock and rock masses, utilizing deep tunnels, cliffs, mountain walls and mountains. In the case of deep tunnels, two empirical methods for assessing the onset of fracturing in massive rock represent the starting point for this wide-reaching exploration of failure modes and the ‘strength’ of rock masses. The classical (Kirsch) formulation is used for estimating the maximum tangential stress $\sigma_{\theta \max}$ in two diametrically opposite locations surrounding an idealized circular tunnel cross-section, excavated or bored in an isotropic elastic medium: ($\sigma_{\theta \max} = 3\sigma_1 - \sigma_3$). This can be compared, following traditional methods, with the unconfined compression strength. However, Shen (see Shen and Barton, 2018) has recently shown that the ratio σ_t/ν (tensile strength/Poisson’s ratio) is the more logical description of limiting strength of rock around a tunnel.

Following this introduction of failure in deep tunnels, the theoretical heights of cuttings and cliffs are evaluated. Here, in place of the Kirsch equations for tangential stress concentrations surrounding circular excavations, we now consider the local principal vertical stress behind a soil cutting or cliff or mountain wall. This can be compared with a measure of the strength of the soil or rock in the same way as before. The likelihood (or not) of failure along an inclined shear surface exiting at the toe of the slope will also be assessed. Both the stability of steep cuttings (in soil) and the stability of sea, river or mountain-wall cliffs in rock might at first sight appear to be governed by conventional Mohr-Coulomb based shear resistance involving cohesion (c) and friction angle (ϕ), but with the necessary differentiation of these strength parameters, to allow for the weakness of soil and the relative strength of most rocks.

Perhaps surprisingly, Mohr-Coulomb based formulations prove to be remarkably unsuitable because rock fails more easily in tension than in shear. The lower-bound solution for cohesion, assuming linear tangents with the σ_t and σ_c Mohr circles, gives estimates of cohesion for typical mountain-wall sandstones and granites that are simply too high to allow failure in shear i.e. a rock avalanche style of failure, unless the vertical walls could be much higher. They usually cannot be, since failure of rock occurs by a mechanism involving extension strain due to Poisson’s ratio, and therefore an ‘earlier’ failure in tension is more likely than eventual shear failure. The anisotropic stress caused by an adjacent free surface is a prerequisite for extension failure overcoming tensile strength.

The application of Mohr-Coulomb shear strength to the failure of rock cliffs and mountain walls is shown in what follows, to *not work* for intact rock, because of the ultra-high cohesion of rock as compared to soils. Consequently, a new approach is tested, using the Shen extension strain criterion ‘in the vertical plane’. An estimate of the major principal stress behind a vertical cliff or mountain wall is all that is needed. For simplicity this is assumed to be γH where γ is the density. So we arrive at the simple criterion: $H_c = \sigma_t/\gamma\nu$.

2 Rock fracturing in deep tunnels

Two empirical methods for assessing the onset of fracturing in deep tunnels in massive rock represent the starting point for this wide-reaching exploration of failure modes and the ‘strength’ of rock masses. Since we will first consider massive or unjointed rock in deep tunnels, we can utilize the classical (Kirsch) formulation for estimating the maximum tangential stress $\sigma_{\theta \max}$ in two diametrically opposite locations surrounding an idealized circular tunnel cross-section, excavated or bored in an isotropic elastic medium: ($\sigma_{\theta \max} = 3\sigma_1 - \sigma_3$).

Table 1 illustrates an SRF (stress reduction factor) table from the Q-system (Grimstad and Barton 1993) for comparison with a later, closely related ‘depth-of-failure’ figure from Martin et al. 1998 shown in Fig. 1a. Table 1 and Fig. 1a are actually telling us the same story from independent sources: expect failure when reaching and passing a maximum tangential stress/unconfined strength ratio ($\sigma_{\theta \max}/\sigma_c$) = 0.4 ± 0.1 m. Thereafter we use elevated SRF ratings if using the Q-system for selecting tunnel support. The photographs in Fig.1 b, c, and d show extension fracture initiation in a TBM tunnel in marble, through to fully developed log-spiral shearing in a sandstone-like model material, as demonstrated when drilling under 3D stress in Addis et al. (1990).

Table 1. The sixth Q-parameter SRF, adjusts the Q-value for the effect of adverse (or benign) ratios of tangential stress in relation to uniaxial strength. Note the rapid increase in the SRF rating when the stress/strength ratio σ_ϕ/σ_c exceeds 0.4. The columns of strength/stress and stress/strength ratios originate from Barton et al. (1974) and Grimstad and Barton (1993).

Competent rock, rock stress problems	σ_c/σ_1	σ_ϕ/σ_c	SRF
H. Low stress, near surface, open joints	>200	<0.01	2.5
J. Medium stress, favourable stress condition.	200 to 10	0.01 to 0.3	1
K. High stress, very tight structure. Usually favourable to stability, may be unfavourable for wall stability.	10 to 5	0.3 to 0.4	0.5 to 2
L. Moderate slabbing after > 1 hour in massive rock.	5 to 3	0.5 to 0.65	5 to 50
M. Slabbing and rock burst after a few minutes in massive rock.	3 to 2	0.65 to 1	50 to 200
N. Heavy rock burst (strain-burst) and immediate dynamic deformations in massive rock	< 2	> 1	200 to 400

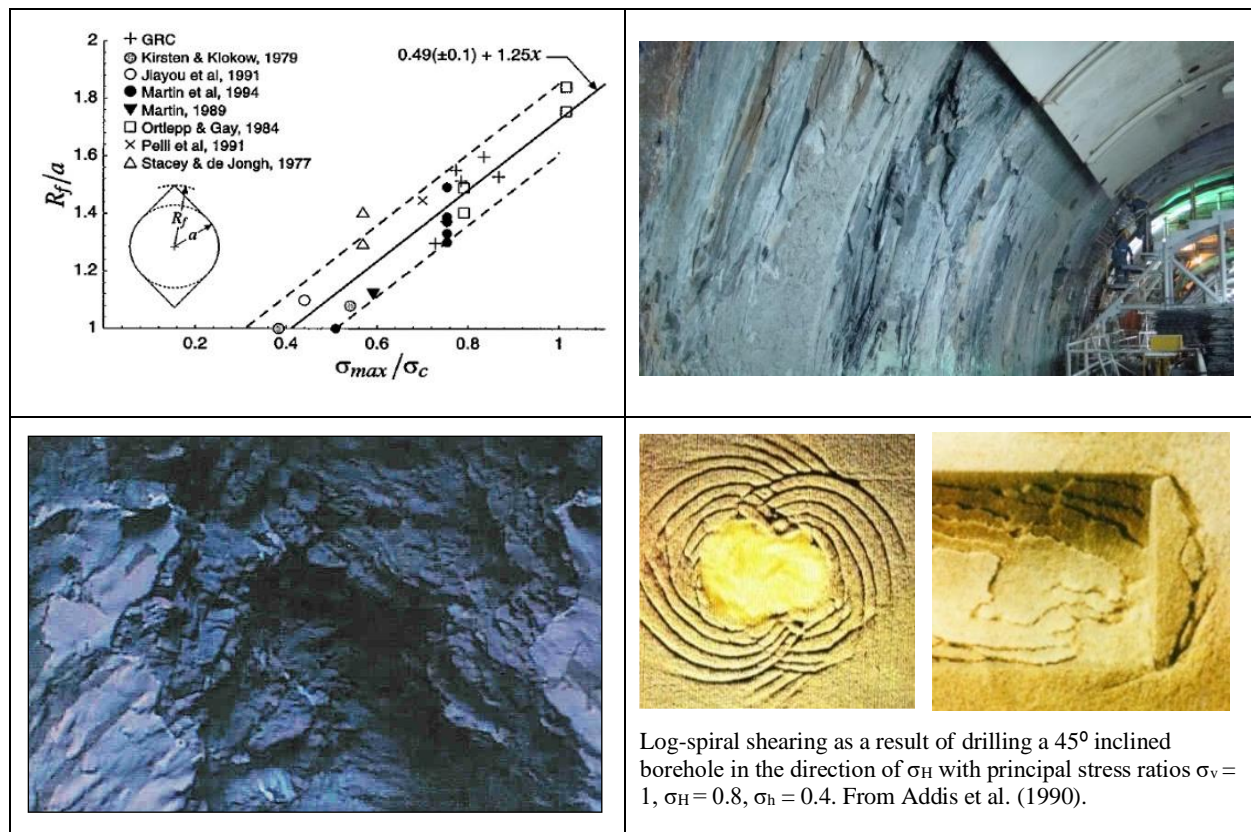


Fig. 1. a). Depth-of-failure data collected by Martin et al. (1998) and others working in deep mining concerning depth of fracturing (R_f -a), suggest the onset of failure when σ_ϕ/σ_c exceeds 0.4 (+/-0.1). This exactly matches the earlier reported experience from deep road tunnels. See 'accelerating' SRF when σ_ϕ/σ_c exceeds 0.4 in Table 1, Grimstad and Barton (1993). b), c). Rock failure initiation and progression to greater depth as extension failure extends into shear in marble and basalt d). Model sandstone: log-spiral shearing caused by boring into high levels of 3D anisotropic stress, as detailed in inset

As will be seen from Fig. 2, the critical tangential stress can alternatively be expressed as σ_t/ν , instead of comparing maximum tangential stress with uniaxial compressive strength. If we assume typical ratios of uniaxial compression/tensile strength (σ_c/σ_t) of 10, and typical values of Poisson's ratio (ν) of 0.25, simple arithmetic shows that the ratio of tensile strength and Poisson's ratio (σ_t/ν) is then equal to $0.4 \sigma_c$. Significantly, this is the same approximate stress/strength ratio seen when acoustic emission begins to increase in laboratory tests. The σ_t/ν criterion (Shen and Barton 2018) is analytically more logical than comparing stress and compression strength because rock will not fail in compression until much higher stresses are reached. Long before this it will have failed in (ex-) tension, with subsequent propagation in shear if stress is further increased, e.g. by nearby mining.

Fig. 2, left, shows an imaginary (green) rock sample in the arch of a deep tunnel, subjected to an almost horizontal maximum tangential stress due to high horizontal principal stress. Extension fracturing can occur close to the tunnel, despite the fact that all principal stresses are positive (i.e. in compression). Dr. Baotang Shen was responsible for noticing the critical stress-strain interpretation which equates the critical tangential stress of $0.4 \sigma_c$ to the alternative ratio σ_t/ν . (See Shen and Barton 2018 for more detail). The simple logic is given in the lower-left panel of Fig. 2.

Fig. 2, top-right shows FRACOD modelling of a ‘stressed’ (and strained) TBM tunnel, with initial extension fractures (red) propagating in shear (green). The massive wall failures in this earliest of TBM tunnels dating from 1880 occurred due to an unusually abrupt increase in stress (+ strain) caused by curving under the 70-90m high Abbots Cliff. A horizontal-to-vertical stress ratio k_o of 1/3 as modelled here, was assumed to be most realistic, in view of the closeness to the cliff face. When k_o was assumed to be 1.0 there was fracturing right around the modelled tunnel, while with k_o of 2 there was concentrated fracturing in the arch and floor of the modelled tunnel. (Barton and Shen 2017).

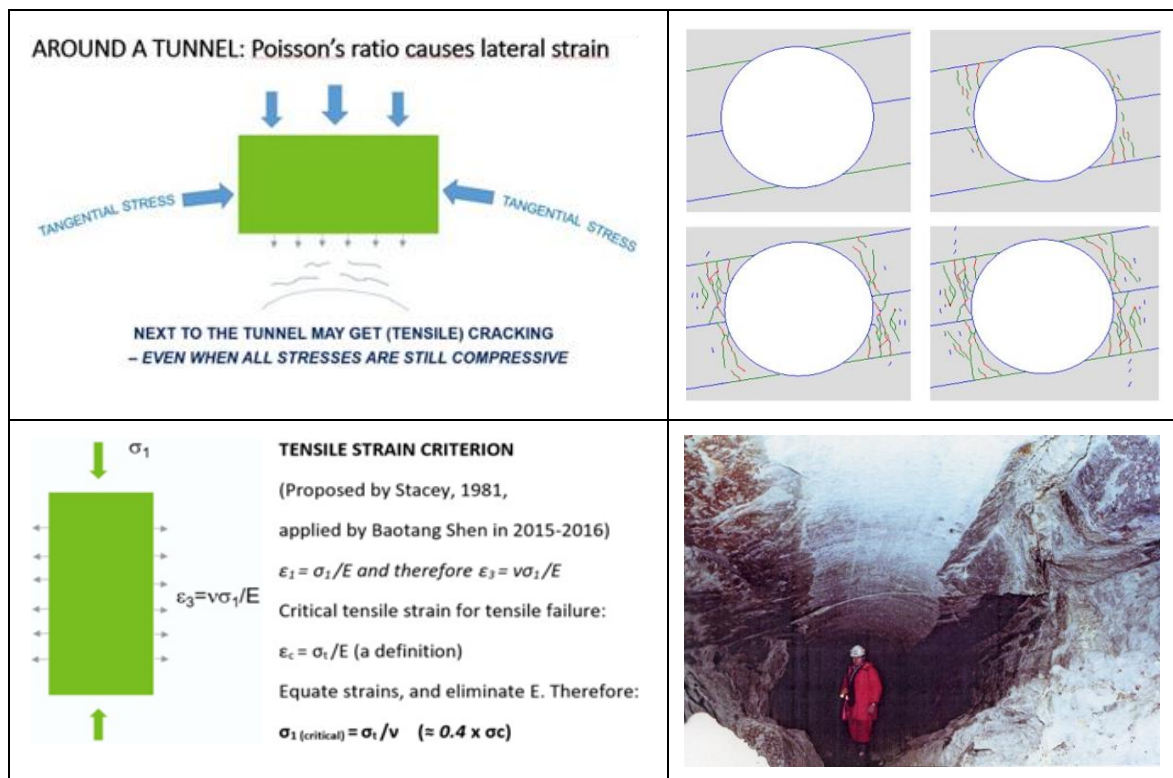


Fig. 2. The extension strain criterion of Dr. Baotang Shen is illustrated by the fracturing and stress-strain logic in the left-hand diagrams. Details can be found in Shen and Barton (2018). On the right, FRACOD modelling performed by Shen shows a fair degree of match to the ‘crushing’ seen when the author visited the Beamont/English tunnel in chalk marl, in order to log Q-parameter statistics for the weak (UCS of 4 to 9 MPa) but distinctly jointed host rock of the UK-France Channel Tunnel. See Barton and Warren (2006, 2019) for details of the Q-logging and comparison with the similar TML consortium Q-logging.

Before leaving underground openings and addressing the strength or strain-limited heights of cliffs and mountain walls, it is appropriate to draw attention to the limitations of conventional continuum analyses, in which one attempts to represent the shear strength of the rock mass by linear (Mohr Coulomb) or non-linear (Hoek Brown) shear strength criteria. Fig. 3 (top) illustrates the Canadian URL mine-by break-out that developed when excavating by line-drilling, in response to the obliquely acting anisotropic stresses.

The central (red) pair of circular tunnel models shown in Fig. 3 are an important demonstration of *unsuccessful modelling* by ‘classical methods’ which were presented by Hajiabdomajid et al. (2000). The conventional modelling was followed with a more realistic degradation of cohesion and mobilization of friction, which was applied in FLAC. A similar approach (degrading cohesion and mobilizing friction) was followed by Pandey and Barton (2011) using FLAC-3D. Pandey used Q-value based input data for c (\approx CC – cohesive component) and ϕ (\approx FC-frictional component) to investigate the over-stress of pre-instrumented (MPBX) and Q-logged mining stopes in India. The CC and FC parameters are obtained by splitting the Q_c formula ($Q_c = Q \times \sigma_c/100$) into two halves (Barton,

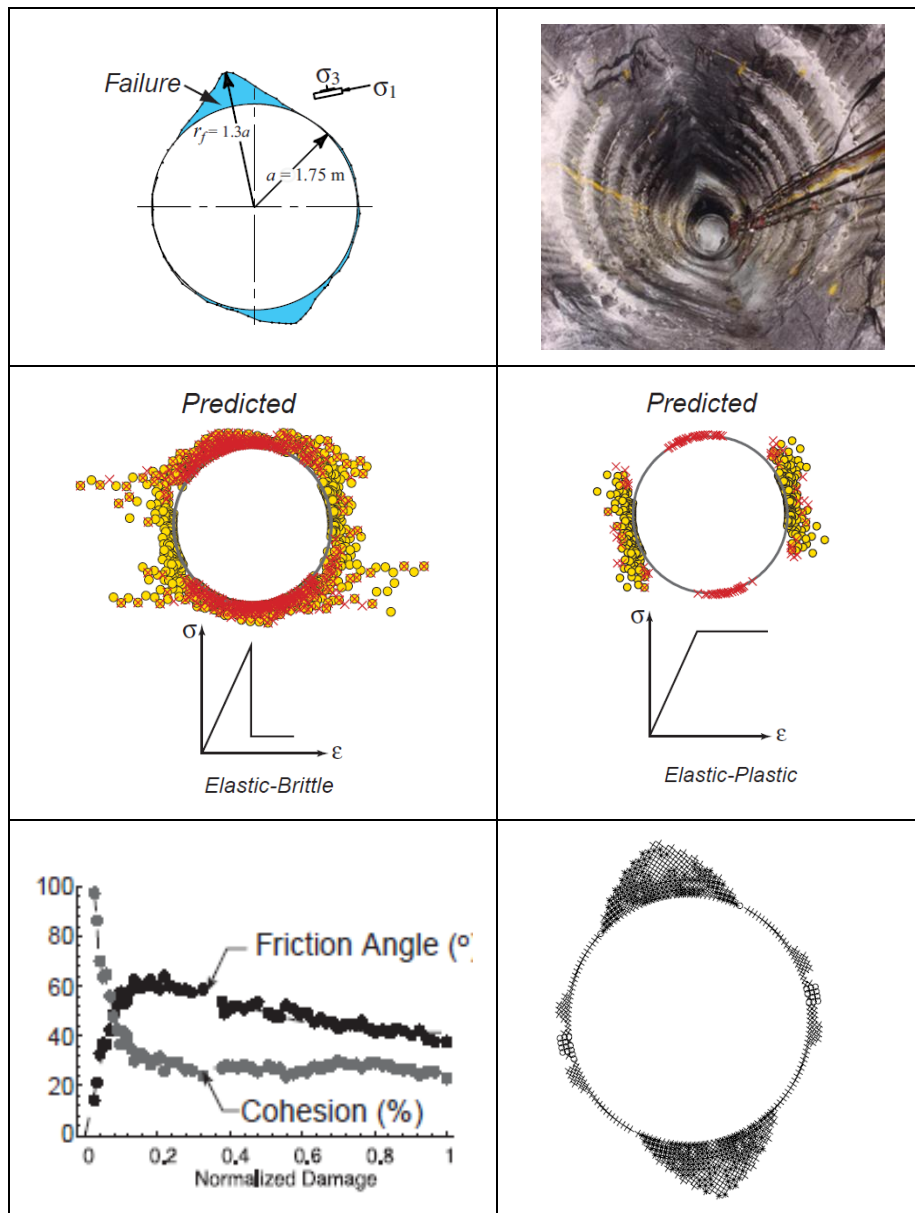


Fig. 3. The remarkable mismatch of continuum modelling with reality, when assuming the convention of adding ‘ c ’ and ‘ $\sigma_n \tan \phi$ ’, whether linear or non-linear, and when considering elastic-brittle and elastic-plastic behaviour. The final pair of figures illustrates the importance of (at least) degrading cohesion and mobilizing friction, as also performed in the land-mark paper of Hajiabdolmajid et al. (2000).

2002). They bear remarkable similarity to the ‘ c and ϕ ’ that are commonly used when modelling rock masses, but were actually derived via the trial-and-error derivation of Q-parameter ratings to fit with shotcrete and bolting needs. (Low CC requires more shotcrete, low FC requires more bolting).

3 Mohr-Coulomb based heights of soil cuttings and rock cliffs

The ‘continued’ mismatch of conventional modelling, involving the addition of cohesive and frictional strength will now be demonstrated, in the context of the limited heights of rock cliffs and mountain walls, where we are generously provided with a huge body of empirical evidence. Nature’s ‘test data’ surrounds us in the mountains and along sea cliffs in the form of *morphological sculpting*, specifically where joint sets *do not* provide the fractured faces of cliffs and mountain walls. That type of failure would be too ‘easy’. The cliff faces and mountain walls would have receded long ago.

We will first consider the stability and failure modes exhibited in the case of cuttings in soil, and then address cliffs (in weaker rock) and mountain walls (in stronger rock). In place of the Kirsch equations for tangential stress concentrations surrounding circular TBM-like excavations, we can now consider the local principal vertical stress behind a cutting or cliff or mountain wall. This can then be compared with a measure of the strength of the soil or rock in the same way as for tunnels.

The likelihood (or not) of failure along an inclined shear surface exiting at the toe of any slope in soil will also be assessed. Both the stability of steep cuttings (in soil) and the stability of sea and river cliffs in rock might at first sight appear to be governed by conventional Mohr-Coulomb based shear resistance involving cohesion (c) and friction angle (φ), but with differentiation of these strength parameters to allow for the weakness of soil and the relative strength of most rocks.

As we shall see, failure of cuttings in soil (which is a granular medium) seem to be better described by a Mohr-Coulomb strength criterion than is possible in (almost) intact rock. The rock is too strong to fail in shear, if it is indeed more or less intact, unless mountain-scale shear stress can be generated by one-to-two thousand meters high mountain walls. But before this rare (rock avalanche) event can happen, an extension strain-related slab failure of massive proportions may already have created a rock climber's Mecca, as for instance in the Yosemite Valley in California, following glacier retreat.

Soil mechanics textbooks show lower-bound and upper-bound solutions for the stability of vertical cuttings in soil, based on c and φ , utilizing the two different assumptions illustrated in Fig. 4. The diversity of the resulting lower-bound and upper-bound solutions, with intermediate results for circular and log-spiral failure surface assumptions already suggests a degree of complexity, which we could add to in rock mechanics, by suggesting (for large-scale slopes) the addition of non-linear shear strength envelopes in contrast to linear Mohr-Coulomb.

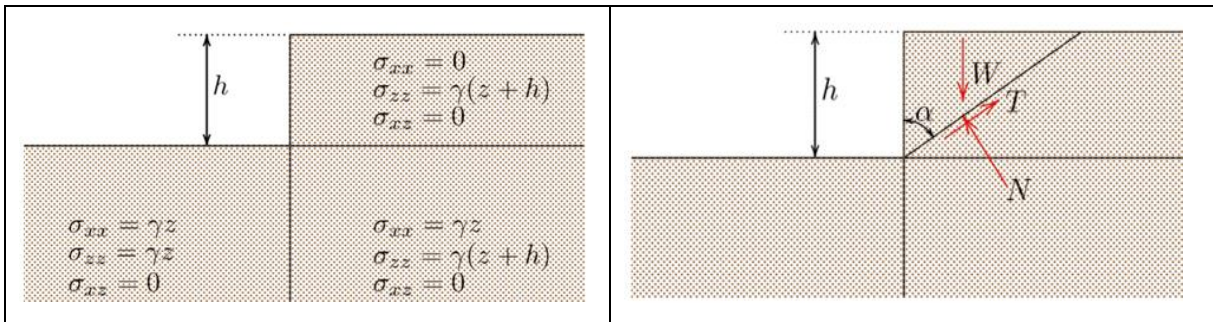


Fig. 4. Left: The equilibrium assumptions for the three zones gives a lower-bound solution. Right: An assumed planar shear surface gives an upper-bound solution. The critical height (h) therefore varies between surprisingly wide margins $4c/\gamma \tan(45^\circ + \varphi/2) \geq h \geq 2c/\gamma \tan(45^\circ + \varphi/2)$. A circular failure surface gives a solution closer to the upper-bound with a multiplier of 3.85. (Verujit 2001).

Equations 1 and 2 summarize the limits of the soil-based criteria. It seems that an exact solution to the vertical cutting problem is elusive, even when utilizing a linear Mohr-Coulomb strength envelope. In the case of high mountain walls, one would need a stress dependent ‘Mohr-Coulomb’ modification. However, as we shall see, the weakest link that actually determines the maximum height of cliffs or mountain walls in (almost intact) rock depends on two entirely different parameters than c and φ .

$$h \geq 2c/\gamma \tan(45^\circ + \varphi/2) \quad (1)$$

$$h \leq 4c/\gamma \tan(45^\circ + \varphi/2) \quad (2)$$

If we do a trial evaluation of potential c and φ values for (assumed) intact rock, using a lower-bound estimate of cohesion from equation 3, we find very quickly that the soil-cutting based solutions of Figure 4 that work moderately well for soil with its relatively low cohesion, *result in far too high values of critical height* (i.e. the maximum possible vertical cliff or mountain wall height) in a range of rocks we are familiar with. Equation 3 is derived from a linear tangent between the uniaxial tension and compression Mohr circles: see later figure.

$$c = 0.5(\sigma_t \cdot \sigma_c)^{0.5} \quad (3)$$

The cohesive strength of intact rock is apparently too high unless the vertical slopes are very high indeed (the mountain avalanche scenario). Experience suggests *alternative failure modes* kicking in at smaller cliff or mountain wall heights. Failure is likely to be due to *extensional strain* causing tensile



Fig. 5. Cliffs in weak materials: tuff in Cappadocia, Turkey and weak inter-bedded sandstone-limestone in Dorset, England. Judging by the surface roughness, these failures cannot be attributed to the opening of vertical jointing. (Such would have caused cliff failures long ago). Suitable estimates of (saturated) rock compressive and tensile strengths, partly based on test results from Aydan and Ulusay 2003 could be the following: Left: Cappadocia cliff, 20m high next to the Christian church, tuff: $\sigma_c = 5\text{MPa}$, $\sigma_t = 0.5\text{MPa}$. Right: Burton cliffs, Dorset 40m high, weak sandstones and limestones. Estimated $\sigma_c = 2\text{MPa}$, $\sigma_t = 0.2\text{MPa}$.

failure, or alternatively the involvement of jointing (if present) and therefore ‘easier’ shear (or joint-opening) failure, obviously giving much lower cliff or mountain wall heights.

The near-vertical cliffs in the weak materials illustrated in Fig. 5 have been given assumed (saturated) strength values in the range $\sigma_t = 0.2$ to 0.5 MPa, and $\sigma_c = 2$ to 5 MPa for simplicity (See caption). Using these ranges of tensile and compression strengths, cohesion strengths (suitably rounded) as low as 0.3 and 0.8MPa can be estimated with the above linear lower-bound envelope. The ratio of the compression to tensile strength Mohr circle diameters generates a presently assumed linear solution for internal friction angle φ as follows: $\sigma_c/\sigma_t = \tan^2(45^\circ + \varphi/2)$. When the ratio of strengths σ_c/σ_t is 10 as assumed for simplicity, this gives $\varphi = 56^\circ$.

The lower-bound soil mechanics-based relationship $h \geq 2c/\gamma \tan(45^\circ + \varphi/2)$ following suitable adjustment of units ($\text{MPa} \times 1000$ for conversion to kN/m^2 so that density can be expressed in kN/m^3) gives predictions of critical cliff heights of approximately 100m and 260m , i.e. far higher than the reality that is probably closer to a $20\text{-}60\text{m}$ range. The upper-bound solutions (equation 2) would be 200m and 520m which are clearly gross over-estimates. For the case of rock, it is all due to the too high cohesive strength of the presently assumed and clearly idealized intact, unjointed rock.

4 Theoretical Mohr-Coulomb based heights of mountain walls

We will now increase the assumptions about the strength of rock in order to attempt to address steep mountain walls in much harder rock, using the same apparently unsuitable Mohr-Coulomb based formulations as outlined in Fig. 4. Again, using deliberately simple numbers, and considering stronger sandstone and granite, we may assume the following approximate ranges of $\sigma_t = 5$ to 10MPa and $\sigma_c = 50$ to 100MPa for the mountain walls illustrated in Fig. 6.

The lower-bound solution for cohesion, assuming linear tangents with the σ_t and σ_c Mohr circles (Equation 3) gives estimates of cohesion for the stronger sandstone and granite of about 8 and 16MPa . These are too high to allow major rock avalanches which would involve the exceedance of shear strength, unless the vertical walls could be much higher. They usually cannot be, since failure apparently has occurred at reduced height, due to different failure mechanisms. The empirical evidence is multiple: the $1200\text{-}1300\text{m}$ maximum heights of the world’s highest mountain walls in (probably) granites or equivalently strong rock. They are well known in rock-climbing literature. These heights have apparently been limited by failure due to extension strain caused by Poisson’s ratio effects, and an anisotropic stress due to the proximity of the respective mountain faces. They will be investigated later and will be compared with reality, and with apparently impossible Mohr-Coulomb solutions.

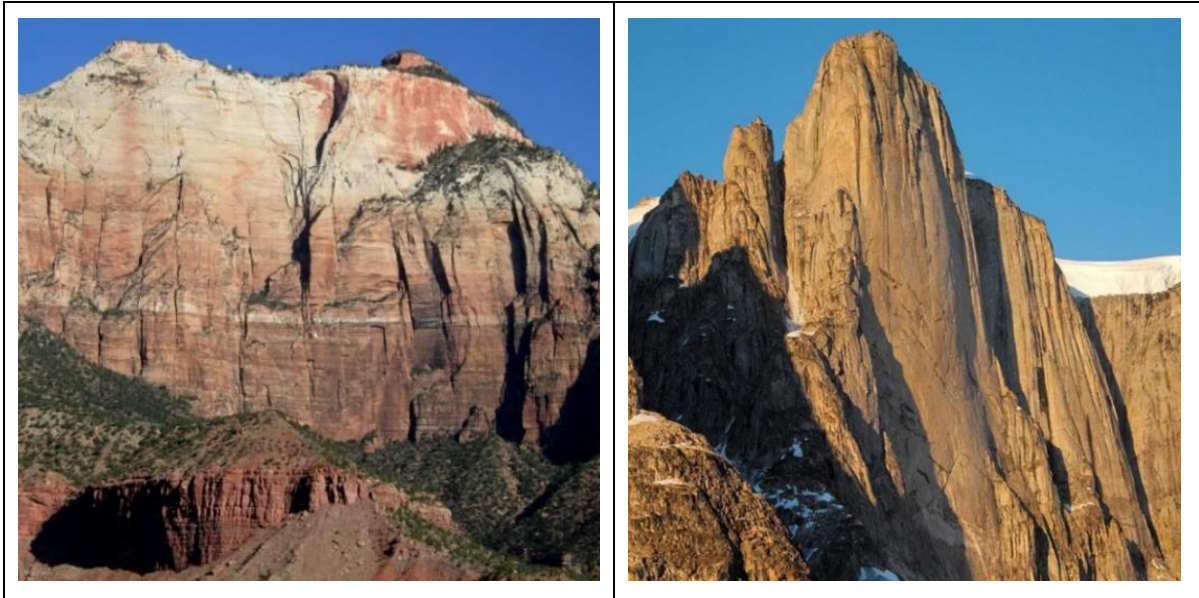


Fig. 6. Mountain walls of almost record height in sandstone and granite are illustrated. Left: West Temple, 750m high, Zion, Utah formed of sandstones, with a conservatively assumed in situ saturated UCS = 50MPa. Right: Mirror Wall, 1,200m high, Greenland which we assume is formed of granite with a conservative in situ saturated UCS = 100MPa.

Using the assumed higher strength values shown in Fig. 6, and tensile/compressive strength ratios of 1/10 again, and the same *lower-bound* soil mechanics based relationship $h \geq 2c/\gamma \tan(45^\circ + \phi/2)$, after suitable adjustment of units (MPa \times 1000 for kN/m^2 and density expressed in kN/m^3), we obtain predictions of critical mountain wall heights of approximately 2070m and 3700m, i.e. far higher than the reality (Fig. 6) that is closer to a 750-1250m range, world-wide, of almost vertical mountain faces.

5 New criterion for the heights of rock cliffs and mountain walls

When assessing the likely onset of failure in deep tunnels (Table 1 and Fig. 1a show the details) the maximum tangential stress and the uniaxial strength were compared, based on the obviously simplifying assumption of isotropic elastic behaviour – but applied nevertheless to explore the onset of fracturing. However, it was found by Baotang Shen (Shen and Barton 2018) that the ratio of tensile strength and Poisson's ratio (σ_t/ν) was a more logical description than the principal stress-induced fracture limit i.e. the well-known fraction of compression strength ($\approx 0.4\sigma_c$). They are almost equal.

Fracturing starts due to extension strain, but this fracturing may propagate in shear, creating classic log-spiral shear surfaces (bottom, Fig. 1b) if stress levels are high enough. Shear failure is usually not possible behind steep mountain walls because stress levels are not high enough, as extension fracturing is likely to initiate when mountain wall heights are much less, when glacial support is lost.

The application of Mohr-Coulomb shear strength to the failure of rock cliffs and mountain walls is clearly not working when using intact rock strength assumptions, because of the ultra-high cohesion of rock as compared to soils. We will therefore test the Shen (σ_t/ν) criterion 'in the vertical plane' (not along a potential shear plane), and simply equate it to an estimate of the major principal stress behind the given vertical cliff or mountain wall. For simplicity we will assume this to be $\sigma_{v\max} = \gamma H$ where γ is the density. Equating the major stress and the Shen failure criterion we obtain for the critical, maximum height H_c the simplest imaginable equation:

$$H_c = \sigma_t/\gamma\nu \quad (4)$$

If we employ strength units of MPa, then the usual vertical stress estimate of $\sigma_v = \gamma H/100$ means that a multiplier of 100 is needed:

$$H_c = 100\sigma_t/\gamma\nu \quad (5)$$

In Table 2 the Mohr-Coulomb derived maximum cliff and mountain wall height estimates (given in blue), are much too high compared with the extension-strain derived critical heights (given in red), based on the simple estimate of maximum vertical stress behind such walls. The red estimates are

Table 2. Comparison of Mohr-Coulomb and extension-strain based critical vertical cliff and mountain wall heights, using common tensile strength and compression strength assumptions.

Lower-bound estimate M-C: $h = \frac{2c}{\gamma} \tan(45^\circ + \frac{\phi}{2})$	Extension strain based: $H_c = \sigma_t / \gamma v$
$\sigma_t = 0.2 \text{ MPa}$ $\sigma_c = 2 \text{ MPa}$ $\gamma = 2.0 \text{ t/m}^3$ $h = 103 \text{ m}$	$\sigma_t = 0.2 \text{ MPa}$ $\sigma_c = 2 \text{ MPa}$ $v = 0.2$ $H_c = 50 \text{ m}$
$\sigma_t = 0.5 \text{ MPa}$ $\sigma_c = 5 \text{ MPa}$ $\gamma = 2.0 \text{ t/m}^3$ $h = 258 \text{ m}$	$\sigma_t = 0.5 \text{ MPa}$ $\sigma_c = 5 \text{ MPa}$ $v = 0.2$ $H_c = 125 \text{ m}$
$\sigma_t = 5 \text{ MPa}$ $\sigma_c = 50 \text{ MPa}$ $\gamma = 2.5 \text{ t/m}^3$ $h = 2067 \text{ m}$	$\sigma_t = 5 \text{ MPa}$ $\sigma_c = 50 \text{ MPa}$ $v = 0.25$ $H_c = 800 \text{ m}$
$\sigma_t = 10 \text{ MPa}$ $\sigma_c = 100 \text{ MPa}$ $\gamma = 2.8 \text{ t/m}^3$ $h = 3690 \text{ m}$	$\sigma_t = 10 \text{ MPa}$ $\sigma_c = 100 \text{ MPa}$ $v = 0.25$ $H_c = 1430 \text{ m}$

more in line with empirical evidence, but perhaps slightly high, suggesting that tensile strength is gradually reduced by the ‘infinite’ number of temperature cycles and wetting and drying cycles in the out-door environment on the surface of, and just behind, these high rock walls. This cycling of temperature does not of course apply in the case of (σ_t/v) extension failure application in tunnels.

We can envisage that the *slab failure* sketched by Melosh (2011) in Fig. 7 (far left) would be a partial simulation of the $\sigma_t/\gamma v$ extension failure mechanism, when occurring in mostly intact massive rock. The *rock avalanche* envisaged by Melosh in Fig. 7 (left of centre) is likely to be a rare event, unless ‘structure’, as sketched in Fig. 8 (left) can develop over extended time, to make reduced areas of ‘rock bridges’ for shear failure to finally be possible. This would counter-act the usually too high cohesive strength of intact rock, as enumerated earlier. It is concluded that the rock avalanche mode is likely to be very rare in the case of massive hard rock, simply because shear stress will usually be insufficient to over-come the ultra-high cohesive strength of intact rock. The condition needed can perhaps be found in high mountains but fortunately is rare.

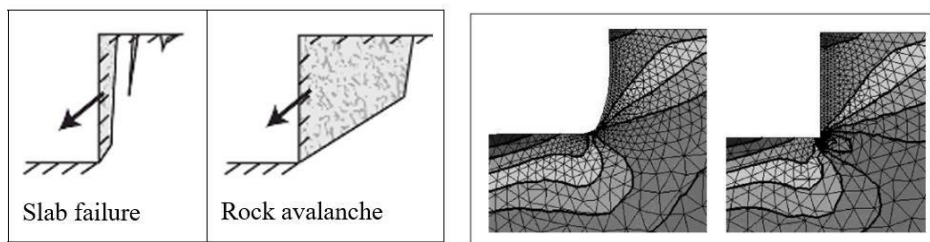


Fig. 7. Left: Two of the failure modes in rock envisaged by Melosh (2011). Right: Two examples of the principal (vertical) stress distribution in the case of near- vertical or vertical walls from Wolters and Müller (2008).

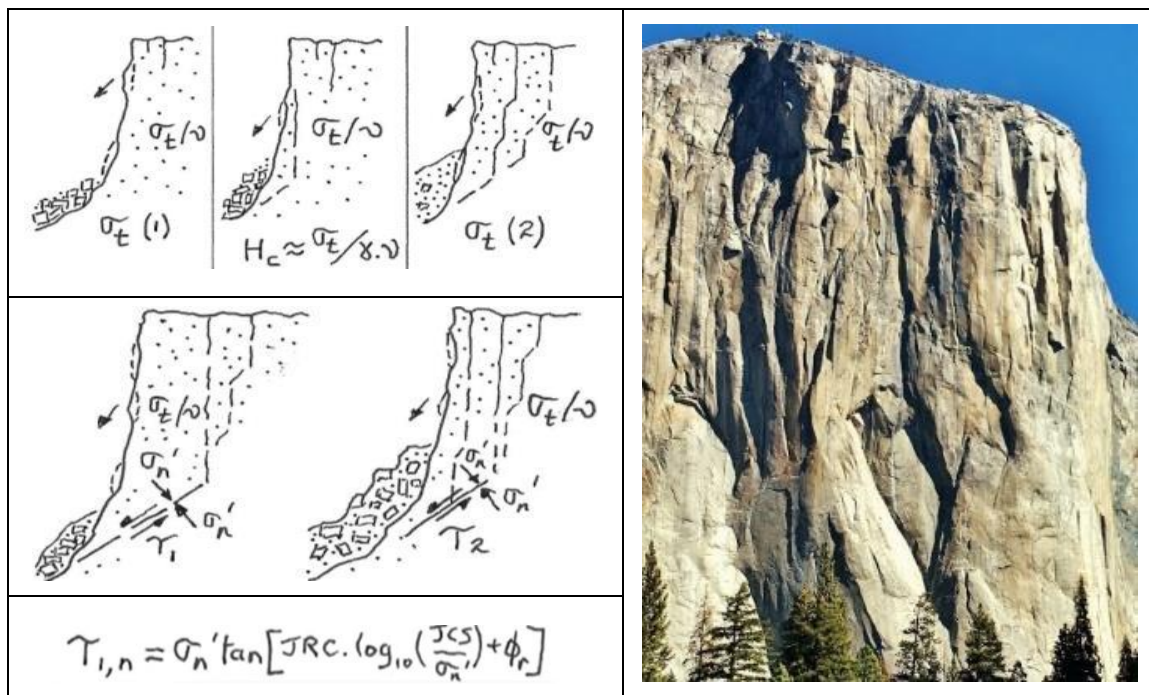


Fig. 8. Left: Sketches of slabbing mechanisms and joint propagation that can be responsible for large scale failures at the front of steep, high, mountain walls. Discontinuous, adversely oriented jointing that is under slope-induced shear stress might gradually propagate. JRC (joint roughness) and JCS (joint wall strength) and ϕ_r (residual friction angle) might finally play an important role in the gradually reducing stability. See ‘whitest’ steep right-dipping plane in the photograph of El Capitan, Yosemite as an example of a partially propagated potential shear plane. It’s depth into the third dimension is unknown but is assumed to be very limited at present.

The details sketched in Fig. 8 include the implication that extension failures cause the slabbing mechanisms that slowly degrade largely unjointed mountain walls. Seasonal and daily temperature variations gradually degrade the tensile strength of the intact rock, while ice-wedging (and joint water pressure) will naturally be the dominant mechanism if discontinuous jointing is already present.

The lower sketch in Fig. 8 explores the possible slow propagation of potential shear failure planes that could allow a rock avalanche to develop, despite a generally too high cohesive strength for the intact rock. In the case of the 950m high El Capitan in Yosemite, a major failure is an extremely remote possibility. This is because the mountain appears largely ‘intact’ beyond and ‘behind’ the famous climber’s ‘Nose’ seen on the right in Fig. 8.

It has been envisaged by those discussing the origin of sheeting joints (e.g. Martel 2017), that their frequent curvature, as seen for instance on the upper half-domed slopes of Half Dome in Yosemite, is due to tensile stress that can be generated by temperature cycling. The curvature-based thermal mechanism is not doubted. However, extension strain mechanisms can act very effectively on planar (i.e. mountain wall) surfaces as well. After all, the principal (vertical) stress is also planar. The cycling of temperature responsible for the gradual reduction of the tensile strength, is an additional and important geomorphological component of failure, aided by Poisson’s ratio.

The world-famous free solo climber Alex Honnold and Steph Davis from the USA (Fig. 9) may be utilizing *extension fractures* rather than *rock joints*, in much of their remarkable free-solo climbing, because rock joints would be likely to have degraded a mountain too quickly when for instance the glacial support (as in cirques) retreated during the last formative ice-age. The extension crack surfaces can be continuous for 100’s of meters, both horizontally and vertically, and can presumably develop in the third dimension if the slope-parallel horizontal stress is limited by a local free face.



Fig. 9. Left: The incomparable Alex Honnold (*Alone on the Wall*, Honnold and Roberts 2016) exploiting (assumed) extension fractures high on El Capitan. Right: USA’s free-solo specialist Steph Davis exploiting extension fracture and joint holds. (Davis 2013. *Learning to Fly: An Uncommon Memoir of Human Flight, Unexpected Love, and One Amazing Dog.*)

The long cracks are the focus of a large number (and size) of rock climber’s *camming* devices for temporarily wedging in these cracks – but finger-tips, fingers, hands, clenched-fists, arms, feet and whole bodies are the ‘cams’ used by the free solo climbers, whose progress is mostly faster without ropes. Refer to Davis (2013), and Honnold and Roberts (2016) for numerous very fine photographs of planar extension fractures, and of course *some* rock joints.

6 Multi-component shear resistance in jointed rock masses

The three strongest shear strength components of a rock mass that is less massive (i.e. more jointed than in Fig. 8) are illustrated in Fig. 10. Shown symbolically as lab tests, they involve the strength of intact rock (the ‘bridges’), followed by shearing along these newly created surfaces, and then mobilization along suitably orientated joints or joint sets. The newly created fractures are likely to have high JRC and high JCS (\approx UCS) and $\varphi_r \approx \varphi_b$ due to a likely lack of weathering. These empirical strength and roughness components were introduced in Barton (1973) and refined in Barton and Choubey (1977). The rock joints will tend to have significantly reduced values of JRC, JCS and φ_r in relation to the fresh fractures. There may be a lesser-magnitude, but very critical fourth component due to clay-bearing faulted rock, represented by a simplified friction coefficient J_r/J_a , using the roughness and clay-filling parameters from the Q-system. These can be quite realistic.

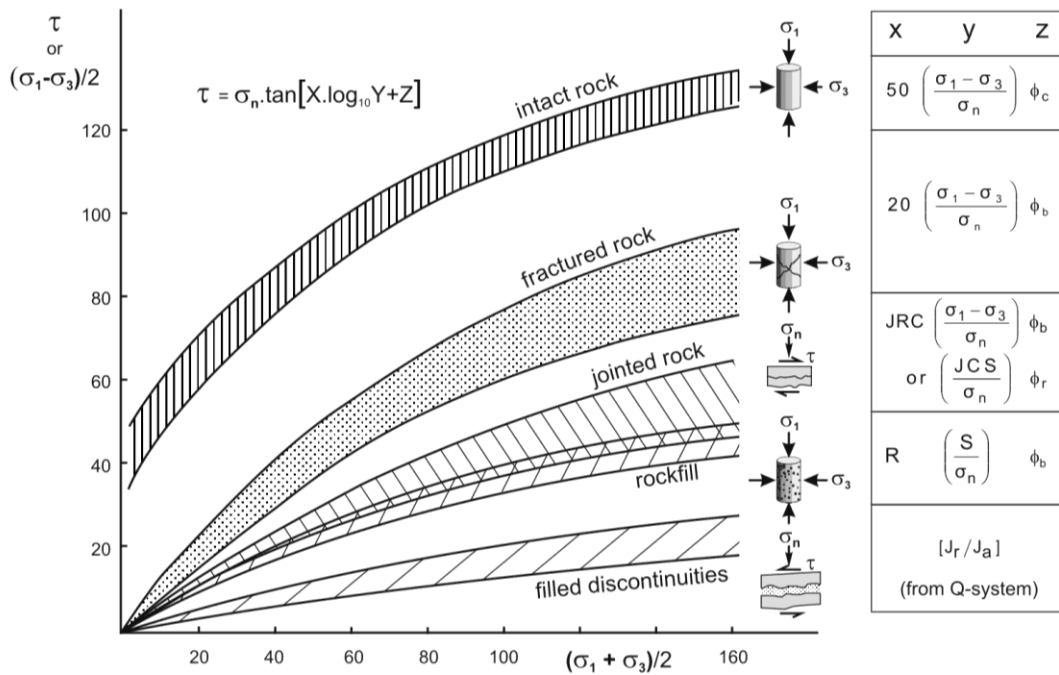


Fig. 10. Four principal shear strength components for cases where rock slope stability is influenced by rock joints, but where sufficient continuity is (presently) lacking, so ‘intact bridges’ and their fracture, and perhaps clay-filled features and/or faults may also be involved. Scale effects will be a source of potential error as very large block sizes inevitably lie outside our experimental data base, and this will affect all attempts at representation. The above components can be remembered as audible: crack, crunch, scrape, swoosh (CCSS). They are reminders of very common progressive failures. (Barton 1999).

Fig. 11 illustrates a famous tourist attraction: Prekestolen (Pulpit Seat) in S.W. Norway, 600m above the Lysefjord. These photographs were kindly provided by Katrine Mo from her comprehensive M.Sc. thesis concerning the geometric mapping and stability analyses of this challenging ‘monolith’. The big question in relation to the theme of *multi-component shear resistance*: will there be initial shear failure or extension failure. Might it be a combination of failure mechanisms?



Fig. 11. Prekestolen, Lysefjord, SW Norway. It is suggested by the present author that shearing on the rear plane, combined with vertical loading due to the tension crack can provide sufficient concentrated vertical stress that failure via extensional strain at the base (white arrow) could be contributory to eventual failure. (Photographs from Katrine Mo, M.Sc.)

Will it be $\tau = c + \sigma_n \tan \varphi$, $\tau = c$ then $\sigma_n \tan \varphi$, $\tau = \sigma_n \tan$ (JRC.log JCS/ $\sigma_n + \varphi_r$), or a possible $\sigma_t/\gamma v$ trigger failure at the base (white arrow) plus two of the above? The principle ‘rock engineering’ components (the joint planes) of Prekestolen are shown in Fig. 11. There is an unusual cyclic ‘micro-loading’ from a widely varying number of probably non-geotechnical, i.e. trusting tourists. (There are sometimes more than 100 tourists on the outermost plateau where five or six can be seen.) However, the seasonal variations including ice-wedging and water pressure in the cyclically blocked joint planes will provide far greater increments of loading. So safer to visit with all the tourists – presumably.

7 The limited height of the world’s highest mountains

There are fifteen mountains in the world with heights in the rarified range of 8 to 9km. The highest of these is Everest at approximately 8,848 masl. The ‘active local height’ is not known. A Wikipedia photograph (extract) is shown in Fig. 12. Since we are concerned with the ultimate strength of rock one can pose the question: why are the highest mountains showing an elevation above sea level no higher than 9km? Have mountains ever been higher than this during the earth’s history? Since plate tectonics has been at work for a very long time, and contrary glacial processes during countless cycles, one can perhaps assume that the extensive ‘empirical evidence’ that we see today is also a reflection of what has been in the distant past. The strength of rock has little reason to have changed either, though it could be higher today, if the geothermal gradient had declined significantly.

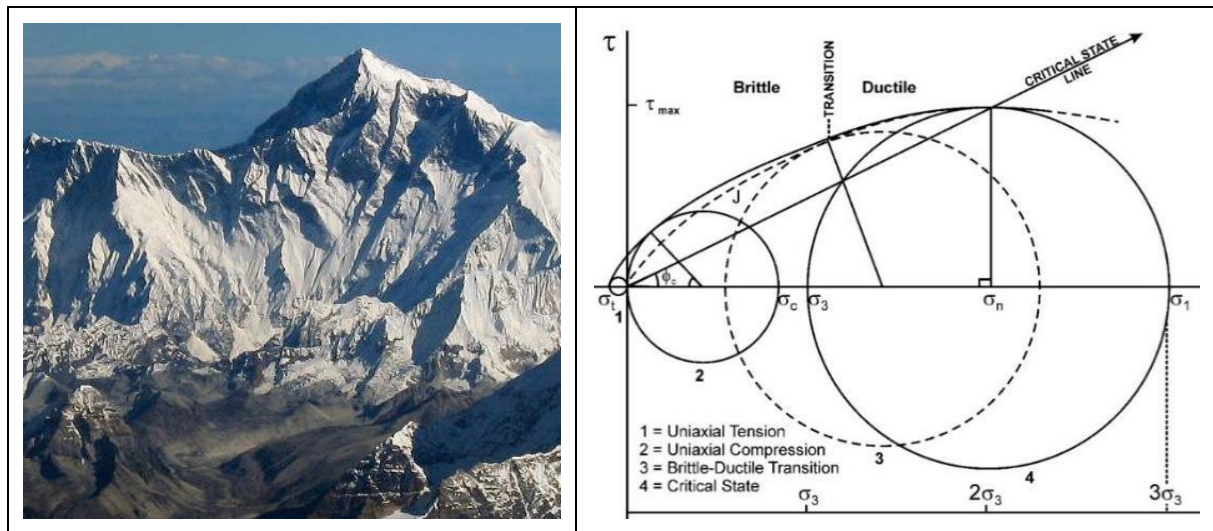


Fig. 12. Left: Mount Everest, 8,864m (Wikipedia photo extract). Note that the peak of Everest is immediately behind the peak showing possible curved ‘shear-planes’. (These cannot be tilted bedding ‘planes’ because of the huge variation in thickness.). Right: The critical state suggestion of Barton (1976). Note the proximity of UCS (or σ_c) and the critical confining pressure σ_3 . Singh et al. (2011) found that σ_c and the critical σ_3 had equal or very similar magnitude.

In a well-known article written by Terzaghi (1962) near the end of his life: ‘*Stability of steep slopes on hard unweathered rock*’, a simple formulation of critical slope height was suggested: $H = q/\gamma$, where the uniaxial strength of rock and the vertical stress caused by its density are compared. The assumed vertical stress was estimated to be γH (or $\gamma H/100$ if using familiar MPa units as in rock mechanics). One can also use units kN/m^2 and kN/m^3 for the rock strength and density.

Misuse of the ‘Terzaghi’ formula: $h_c = \sigma_c/\gamma$ (equation 6) gives an apparently correct answer for maximum mountain heights (e.g. $100 \times 250/2.8 = 8.9\text{km}$ (with $\sigma_c = 250\text{MPa}$). The problem is that it has to be the *confined strength* of rock at 9 km depth, and this is three times too high to produce a believable maximum mountain height. (We fortunately do not experience 25km mountain heights).

$$h_c = \sigma_c/\gamma \quad (6)$$

This formula was not evaluated in the section concerning limited cliff heights and mountain walls since it (also) produces a strongly exaggerated result, and Terzaghi was quick to point out in his 1962 article that the adverse effect of jointing must be the reason that ‘critical slope heights’ were not in practice as high as this formula was suggesting. The reason (besides jointing) is that in the case of massive intact rock, there are alternative mechanisms of rock failure: possibly even shear failure when stress levels are high, but never mobilization of *unconfined* compression strength beneath a mountain.

Application of a typically high value of uniaxial compression strength of rock in the case of ultimate mountain height estimation is a ‘popular’ method that is also shown in a Google ‘chat-site’. The problem is that the rock involved in ‘stabilizing’ the vertical effective stress generated by the mountain, cannot possibly be the unconfined strength at e.g. 9km depth. It must be the *confined* compressive strength.

Correct logic actually suggests that mountains are of ‘limited’ height due to a lower (critical state) shear strength, which may also be approximately 200-250 MPa. Inspection of Figures 12 gives simple confirmation that the indicated value of σ_1 (see right-hand side of largest Mohr circle) would be much too high in relation to (unconfined) σ_c . On the other hand, the maximum shear strength is of similar magnitude (almost equal) to the uniaxial strength. (See Barton, 1976, Singh et al. 2011, Singh and Barton, 2019 and Shen et al. 2019). Observation of the strong curvature of the shear strength of intact rock at high confining pressure (e.g. Mogi 1966) as reviewed by Barton (1976), was the reason for proposing a maximum possible shear strength and thus simply defining the critical state (Figure 12).

The *consequences* of the strong curvature of shear strength envelopes, actually a significantly stronger curvature than that of the Hoek-Brown criterion for intact rock, have been further investigated by Shen et al. (2018), who demonstrated with the FRACOD fracture mechanics code that a somewhat larger volume of rock would be fractured as a result of tunnel siting at 1 or 2km depth, as compared to the fractured volume modelled with conventional (M-C, H-B) models of shear strength. Shen et al. (2018) formulated relatively simple equations with recognizable input parameters, to describe both the tensile and compressive sides of the non-linear shear strength envelope, for a result very similar to Fig. 12b.

8 Conclusions

1. Tensile strength and Poisson’s ratio explain the limited maximum heights of cliffs and steep mountain walls, and the origin of planar sheeting joints. A range of maximum heights from 20m in tuff, 100m in chalk, 750m in sandstone, to 1,300m in granite can be sensibly quantified by considering failure caused by extensional strain in each case. Mohr-Coulomb shear strength parameters give incorrect and greatly exaggerated results for intact rock, in the context of these ultra-steep slopes.
2. There are parallels in the world of deep tunnels in hard rock. The widely quoted critical tangential stress of $0.4 (\pm 0.1) \times \text{UCS}$ that may signal the onset of ‘stress-induced’ fracturing in deep hard rock tunnels can be more correctly replaced by the ratio σ_t/ν , representing initial tensile failure which is caused by exceeding the critical extensional strain. These two ratios are numerically equivalent. At higher stress levels, tensile fractures may propagate in unstable shear, meaning potential rock bursts. UCS per se is not involved in failure in tunnels, while it may be in laboratory tests, though here also, tensile and shear failure are often involved when testing intact rock cylinders.
3. Shear strength and tensile strength *respectively*, the latter ably assisted by Poisson’s ratio, are inevitably the weakest links in ‘high-stress’ structural geology and in ‘low-stress’ geomorphology.
4. Rock slopes with discontinuous rock joints may reach failure if several shear strength components are mobilized/over-come one-by-one in a *progressive* manner. Recall ‘crack, crunch, scrape, swoosh’ as sonic reminders of a likely non-Mohr-Coulomb non-Hoek-Brown progressive failure (CCSS) event.
5. The highest mountains of 8 to 9km are most likely to be limited by maximum possible *critical state shear strength*, not by compressive strength, because the necessary confined compressive strength of competent mountain-forming rock is at least three times too high. Mountains cannot be 25km high.
6. There is natural uncertainty about the ‘equilibrium depth’ beneath a mountain chain, and also about the effective pore pressure when there are frozen peaks and deep permafrost. Drainage to nearby valleys is also unknown. If the ‘local’ mountain load is in equilibrium with the resisting (shear) strength at say 5 to 6km depth, then a scale effect on shear strength is implied and is also logical.

9 References

Addis MA, Barton N, Bandis SC, Henry JP (1990) Laboratory studies on the stability of vertical and deviated boreholes. 65th Annual Technical Conference and Exhibition of the Society of Petroleum Engineers, New Orleans, September 23-26, 1990.

- Aydan Ö, Ulusay R (2003) Geotechnical and geo-environmental characteristics of man-made underground structures in Cappadocia, Turkey. *Engineering Geology*, 69, 245-272.
- Bandis S, Lumsden AC, Barton N (1983) Fundamentals of rock joint deformation. *Int. J. Rock Mech. Min. Sci. and Geomech. Abstr.* Vol. 20: 6: 249-268.
- Barton N (1973) Review of a new shear strength criterion for rock joints, *Engineering Geology*, Elsevier, Amsterdam, Vol. 7, pp. 287-332.
- Barton N, Lien R, Lunde J (1974) Engineering classification of rock masses for the design of tunnel support. *Rock Mechanics*. 6: 4: 189-236.
- Barton N (1976) The shear strength of rock and rock joints. *Int. Jour. Rock Mech. Min. Sci. and Geomech. Abstr.*, Vol. 13, No. 9: 255-279.
- Barton N, Choubey VC (1977) The shear strength of rock joints in theory and practice. *Rock Mechanics* 1/2:1-54. Vienna: Springer.
- Barton N, Warren C (1996) Rock mass classification of chalk marl in the UK Channel Tunnels. *Channel Tunnel Engineering Geology Symposium*, Brighton, September 1995.
- Barton N (1999) General report concerning some 20th Century lessons and 21st Century challenges in applied rock mechanics, safety and control of the environment. *Proc. of 9th ISRM Congress*, Paris, 3: 1659-1679, Balkema, Netherlands.
- Barton N (2002) Some new Q-value correlations to assist in site characterization and tunnel design. *Int. J. Rock Mech. & Min. Sci.* Vol. 39/2:185-216.
- Barton N, Grimstad E (2014) Q-system - an illustrated guide. 43p. www.nickbarton.com.
- Barton N, Shen B (2017) Extension failure mechanisms explain failure initiation in deep tunnels and critical heights of cliff faces and near-vertical mountain walls. *US Rock Mech. Symp. San Francisco, ARMA17*, 20p.
- Barton N, C Warren (2019) Rock mass classification of chalk marl in the UK channel tunnels using Q. Ch. 18. *Soft Rocks Mechanics and Engineering*. Eds. Kanji, He, & Sousa. Springer.
- Davis S (2013) *Learning to Fly: An Uncommon Memoir of Human Flight, Unexpected Love, and One Amazing Dog*. A Touchstone Book, Simon & Schuster, New York, 292p.
- Grimstad E, Barton N (1993) Updating of the Q-System for NMT. *Proc. of Int. Symp. on Sprayed Concrete – Modern Use of Wet Mix Sprayed Concrete for Underground Support*, Fagernes, 1993, Eds Kompen, Opsahl and Berg. Norwegian Concrete Association, Oslo, 46-66.
- Hajiabdolmajid V, Martin CD, Kaiser PK (2000) Modelling brittle failure. *Proc. 4th North American Rock Mechanics Symposium, NARMS 2000 Seattle*. J. Girard, M. Liebman, C. Breeds and T. Doe (Eds), 991–998. A.A. Balkema, Rotterdam.
- Honnold A, Roberts D (2016) *Alone on the Wall*. W.W. Norton & Company, New York. 248p.
- Martel SJ (2017) Progress in understanding sheeting joints over the past two centuries. *Jour. of Structural Geology*, Elsevier, 94, 68-86.
- Melosh HJ (2011) *Planetary surface processes*. Cambridge University Press, Cambridge. *Geology*, Elsevier, 94, 68-86.
- Martin CD, Kaiser PK, McCreath DR (1998) Hoek–Brown parameters for predicting the depth of brittle failure around tunnels. *Can. Geotech. J.* 36, 136-151.
- Mo K (2018) *Stability Analysis of Preikestolen*. M.Sc., *Engineering Geology*, NTNU, Trondheim.
- Shen B, Barton N (2018) Rock fracturing mechanisms around underground openings. *Geomechanics & Engineering*, Techno-Press, Ltd. V.16, No. 1, 35-47.
- Shen B, Shi J, Barton N (2018) An Approximate Non-Linear Modified Mohr-Coulomb Shear Strength Criterion with Critical State for Intact Rocks. *J. of Rock Mech. and Geotech. Eng.* 10 (2018) 645-652.
- Singh M, Raj A, Singh B (2011) Modified Mohr-Coulomb criterion for non-linear triaxial and polyaxial strength of intact rocks. *Int. J. Rock Mech. Min. Sci.*, 48(4), 546-555.
- Singh, M. and N. Barton, 2019. Highest Mountains Suggest Strong Curvature of Shear Strength Envelopes for Rock. *Proc. of ISRM Cong. Foz do Iguacu, Brazil*.
- Stacey TR (1981) A simple Extension Strain Criterion for Fracture of Brittle Rock. *Int. J. Rock Mech. Min. Sci. & Geomech. Abstr.* 18, 469-474.
- Terzaghi K (1962) Stability of steep slopes on hard unweathered rock. *Geotechnique* 12:251-263.
- Verruijt A (2001) *Soil Mechanics*. Delft University of Technology, The Netherlands.
- Wolters G, Müller G (2008) Effect of cliff shape on internal stresses and rock slope stability. *J. Coastal Res.* 24(1), 43-50, Florida.